We are IntechOpen,
the world's leading publisher of
Open Access books
Built by scientists, for scientists

6,900
Open access books available

185,000
International authors and editors

200M
Downloads

154
Countries delivered to

Our authors are among the

TOP 1%
most cited scientists

12.2%
Contributors from top 500 universities

BOOK CITATION INDEX
CLARIVATE ANALYTICS
INDEXED

WEB OF SCIENCE™

Selection of our books indexed in the Book Citation Index
in Web of Science™ Core Collection (BKCI)

Interested in publishing with us?
Contact book.department@intechopen.com

Numbers displayed above are based on latest data collected.
For more information visit www.intechopen.com

Failure Analysis of a High-Pressure Natural Gas Heat Exchanger and its Modified Design

Lei-Yong Jiang, Yinghua Han, Michele Capurro and
Mike Benner

Additional information is available at the end of the chapter

Abstract

The beauty of numerical simulations is its ability to reveal the physics or nature of practical engineering problems in detail, and then, to identify adequate solutions. In this chapter, an excellent example is demonstrated. The rupture of a heavy-duty, high-pressure natural gas heat exchanger is numerically investigated, and the importance of gravity effect is identified, which is often considered as a trivial factor. For the original design, the natural convection in the flow field of the heat exchanger is comparable with the forced convection at the designed operating conditions. These two convections are perpendicular and compete with each other, the flow field is highly unsteady, and high-temperature natural gas is trapped in the upper portion of the vessel, which causes the damage of the exchanger. By vertically mounting the exchanger assembly and locating the outlet pipe on top of the exchanger, the flow parameters become rather uniform at each vertical cross section and the wall temperature of the heat exchanger remains more or less the same as the heated natural gas. The proposed design has been successfully used up to now.

Keywords: forced convection, natural convection, heat transfer, heat exchanger, turbulent diffusion

1. Introduction

The beauty of numerical simulations is its ability to reveal the detailed phenomena or nature of complicated practical engineering problems, which are difficult and sometimes impossible from experimental studies. Based on the obtained numerical results, adequate solutions can easily be identified.
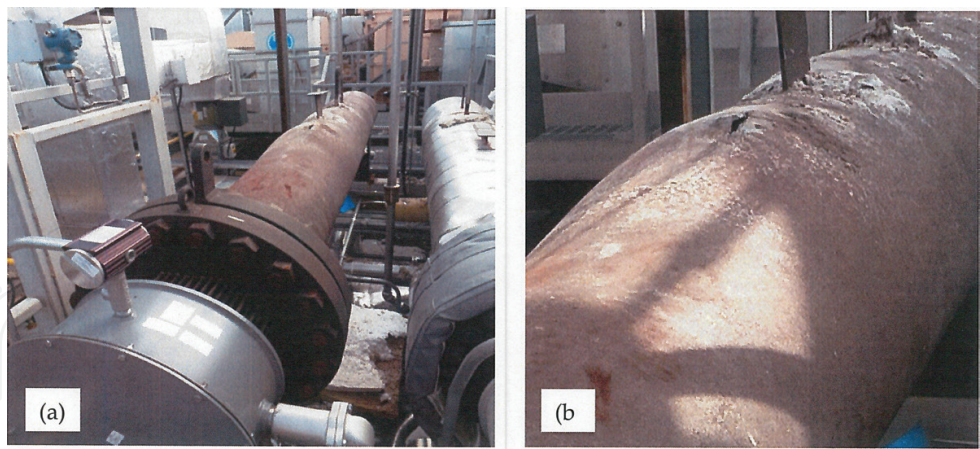
Figure 1. The natural gas heat exchanger: (a) the damaged heat exchanger; and (b) a close view of the cracks on the top surface of the vessel.

This chapter gives an excellent example for this type of approaches. To identify the reasons for the rupture of a heavy-duty, high-pressure natural gas heat exchanger, as shown in **Figure 1**, the flow field of the heat exchanger was numerically examined. Based on the findings, a new configuration was suggested and the corresponding flow field was studied. The installed modified heat exchanger has been trouble-free used to date. In the following sections, the computational domain, mesh, numerical methods, flow features of the two designs, and the cause of the heat exchanger damage are presented and discussed.

2. Numerical simulations

2.1. Computational domain and mesh of the original design

The natural gas heat exchanger has a nominal power of 390 KW, and the effective length of its heavy-duty vessel is 3785 mm with an outside diameter of 457.2 mm. As a sketch shown in **Figure 2**, it accommodates 138 (276 rods) heating elements. The diameter of these elements is 10.9 mm, and the length is 3277 mm for 64 long elements and 3252 mm for 74 short elements.
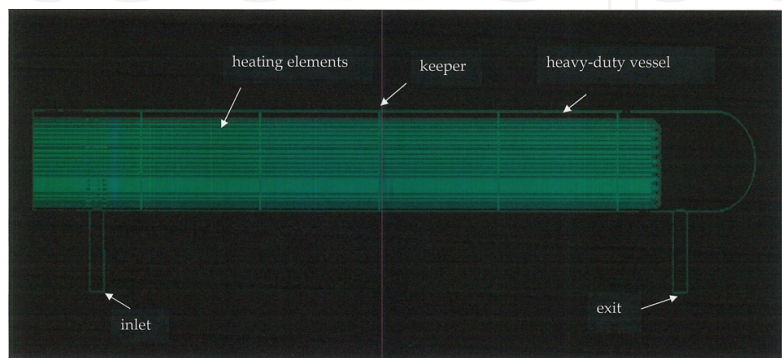

Figure 2. The computational domain of the original design.

Five keepers are inserted inside the vessel to maintain the proper radial positions of these elements. The nominal diameter of the inlet and exit pipes is 80 mm. The computational domain covers the whole flow field of the heater from the inlet to the exit, including heat elements and five keepers. It is important to mention that the whole natural gas heat exchanger assembly was mounted horizontally.

The mesh for one section of the heat exchanger vessel is shown in **Figure 3(a)**, and the mesh at a cross section cutting through heating elements is illustrated in **Figure 3(b)**. In these two plots, the meshed areas are where the natural gas flows, and the unmeshed hollow regions or circles are where the heating elements are located. **Figure 3(c)** is the mesh cutting through one keeper. As shown in **Figure 3(c)**, there are hundreds of small holes (11.5 mm in diameter) on the perforated plate of the keeper, 276 holes are considered blocked by the heating elements, and the rest meshed are flow passages. A narrow annular flow channel surrounding the keeper is used to keep the heating elements away from the vessel inner surfaces. Adjacent to the annular flow channel, parts of full circles are cut out by a flat bar of the keeper. The mesh size is ~4.0 million in the number of cells.

2.2. Boundary conditions

The inlet boundary conditions for the numerical simulations are listed in **Table 1**.

The heavy-duty vessel was wrapped with insulation material, and so it was reasonable to assume adiabatic boundary condition for its external wall boundaries. A heat flux of 4.48 KW/m^2 was specified at the heating-element surfaces starting from the middle cross section of the inlet pipe to the end of the heater elements. An increase in natural gas temperature by ~200 K, from the room temperature, was expected. In the investigation, the natural gas was considered as pure methane.

2.3. Numerical methods

Steady, turbulent, thermal flows were considered in the present work, and a commercial software package, Fluent, was used for all simulations. The governing Favre-averaged conservation equations of mass, momentum, and enthalpy are not reproduced here, but can be readily found in [1, 2].

For closure of these partial differential equations, the realizable k-ε turbulence model was applied to model turbulent momentum transfer. A benchmark study on turbulence models indicated that this model was superior to other four popular two-equation models and could provide similar results as those from the Reynolds stress model, a second-momentum closure [3]. The Reynolds analogy [4] was used to account for turbulent enthalpy transfer, and for this type of pipe flows, the turbulence Prandtl number of 0.7 was used [5, 6]. The gravity of 9.8 m/s^2 was assigned in the direction consistent with the heat exchanger mounting orientation.

For the thermal properties of methane, polynomials derived from the NIST JANAF tables [7] were used to calculate the specific heat as a function of temperature. Data from NIST [8] were used to obtain polynomials to determine the molecular viscosity and thermal conductivity of methane as functions of temperature.
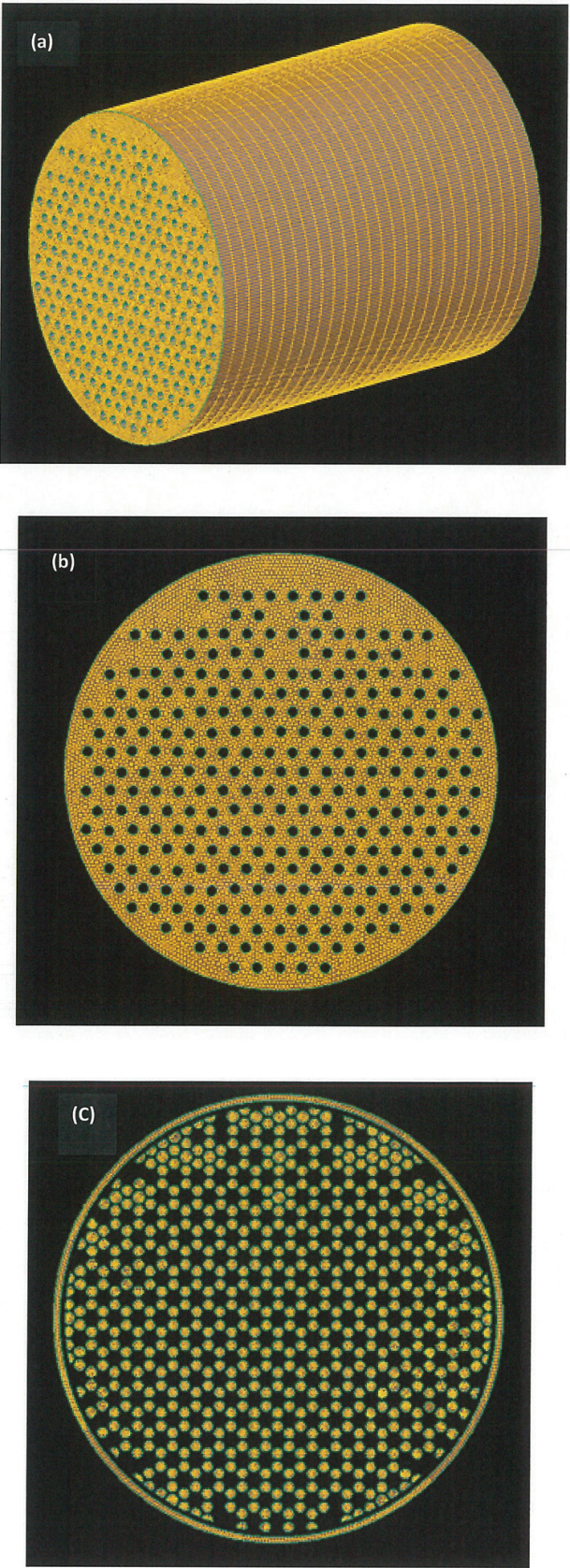
Figure 3. Meshes: (a) mesh for one section of the heat exchanger; (b) mesh at the section across heating elements; and (c) mesh across one heating-element keeper.

Mass flow rate	0.237 kg/s
Temperature	295.3 K
Absolute pressure	30.4 bar

Table 1. The inlet boundary conditions.

A segregated solver with a second-order accuracy scheme was chosen to resolve the flow fields. At convergence, the imbalance of mass flow rate between the inlet and exit was less than 0.34% for the original design and 0.007% for the modified configuration, while for the energy imbalance it was 0.38% for the former and 0.007% for the later. Due to the unsteady nature of the thermal flow field of the original design, the convergence could not reach the level for the modified case. Sixteen cores of a 64-bit LINUX cluster with 4 GB RAM for each core were used to perform all simulations.

3. Results and discussion

3.1. Results of the original design

Figure 4 shows the temperature contours along the longitudinal symmetric plane of the heat exchanger. Significantly, variation of temperature inside the heater is observed. High-temperature region exists in the upper portion of the vessel, while the low-temperature regions occur in the lower portion. The temperature profiles along the top and bottom walls are displayed in **Figure 5**. It is obvious that the top wall temperature reaching ~1700 K is considerably higher than the allowed service temperature of steel pipes, SA-106 GR.B [9]. Certainly, the heavy-duty vessel could not survive at such high-temperature and high-pressure operating conditions. Another important feature in **Figure 4** is the unsteady nature of the thermal flow field. Large eddies or fluid pockets randomly occur in the regions along and above the central axis of the vessel.

Why is the vessel wall temperature so high when the natural gas is set to be heated by only ~200 K? And why is the thermal flow field so unsteady in nature? These questions can be answered by analyzing the flow features or characteristics inside the heat exchanger vessel.
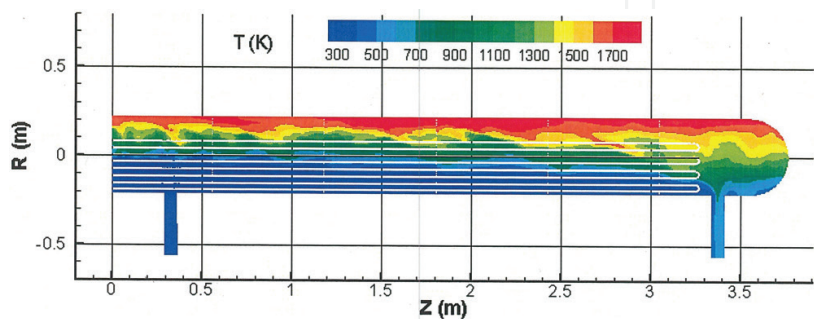

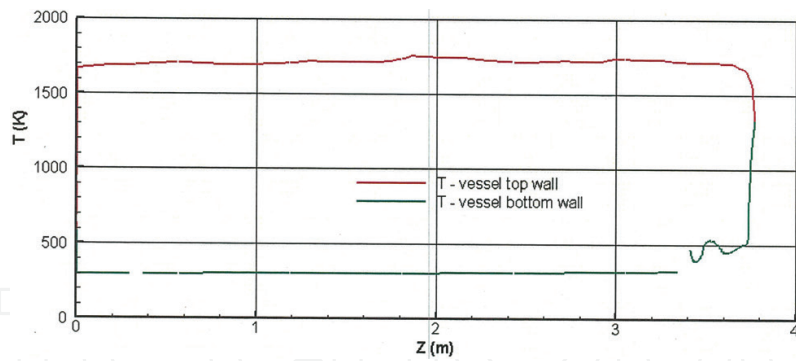**Figure 4.** Temperature contours at the longitudinal symmetric plane.

Figure 5. Temperature profiles along the vessel top and bottom walls.

The first or primary cause for the heat exchanger damage is that the forced convection in the flow field is weak, the natural convection is strong and comparable with the former, and these two actions are perpendicular and compete with each other. **Figure 6** is the velocity magnitude contour plot across the symmetric plane. As observed, the velocity inside the heater vessel is low, the mean velocity magnitude over the whole domain is only 0.174 m/s, and the mean Reynolds number is ~2800. This means that the forced convection mainly in the longitudinal direction is weak. The absolute pressure distribution in the vessel is shown in **Figure 7**, and it varies a little around 3.04×10^6 Pa.

The methane density contours at the symmetric plane are shown in **Figure 8**. The density changes dramatically inside the heat exchanger vessel. High-density regions appear in the inlet pipe and lower portion of the vessel, and the maximum value reaches 20 kg/m³, while the low-density regions happen in the upper portion of the vessel with a minimum of 3.0 kg/m³. Due to the gravity, large differences in density induce strong natural convection inside the vessel.

As shown in **Figure 4**, the unsteady flow feature, randomly distributed flow pockets, is also observed in **Figure 8**. Velocity vectors at the portion of the symmetric plane are illustrated in **Figure 9**, where the vessel and keeper walls are indicated by blue lines, the length of vectors represents the magnitude of local velocities, and for comparison a reference vector of 0.2 m/s is provided. As shown in **Figure 9**, large counterclockwise recirculation regions are formed in the upper half of the vessel, which are induced by the relatively high horizontal velocities in the
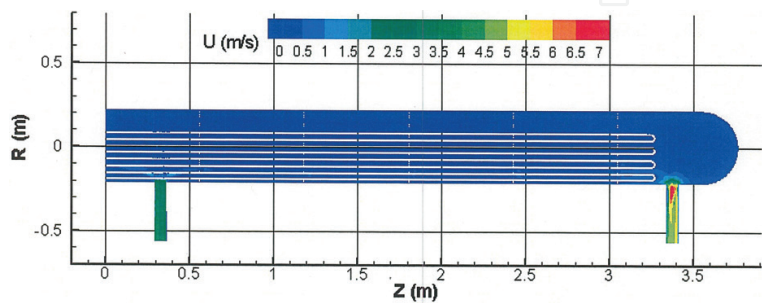

Figure 6. Velocity contours at the longitudinal symmetric plane.
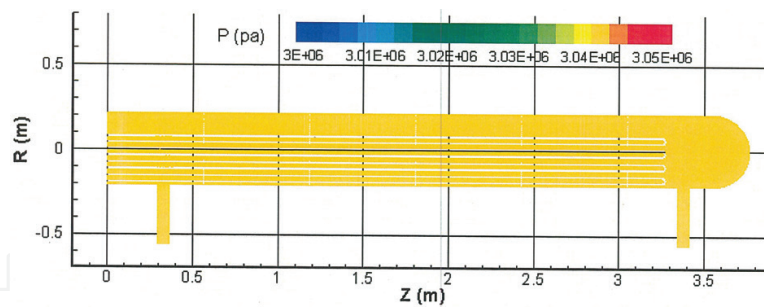
Figure 7. Absolute pressure contours at the longitudinal symmetric plane.

lower half of the vessel. The vertical velocity component corresponding to the natural convection is comparable with the horizontal component related to the forced convection. As a result of the competition between the two convections, the flow field inside the vessel becomes unstable in nature. The gas temperature at one point in the high-temperature region can vary by ±80 K.

These observations are consistent with a first-order analytical assessment in Ref. [10]. As stated in the book, when the ratio of R = Gr/(Re)^2 ≈ 1, the combined forced and natural convections must be considered in heat transfer analysis. Here, Gr is the Grashof number and Re stands for Reynolds number. Based on the averaged values of flow parameters, this ratio equals to 0.6 for this case.

Figures 10–13 provide detailed distributions of temperature and velocity magnitude at the inlet, outlet, and four middle cross sections, and at the five keeper cross sections, respectively. These plots further confirm the above observed flow features. The high-temperature region occupies about one-third of the cross-sectional areas, and the low-temperature region gradually decreases from half of the area at the inlet section, to about one-third of the area at the last keeper section, and eventually a fraction at the outlet section (**Figures 10** and **12**). As observed in **Figures 11** and **13**, the velocity magnitude in the lower halves at these cross sections is higher than that in the upper halves.

The second reason for the heat exchanger damage is that the flow exit is located at the lowest position of the whole flow domain (**Figure 2**). Consequently, the high-temperature or low-density fluid is trapped in the upper portion of the vessel, does not flow out of the vessel, and keeps recirculating, as shown in **Figures 9** and **14**.
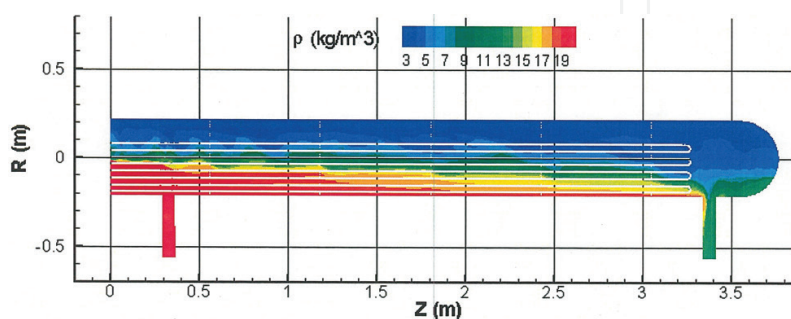

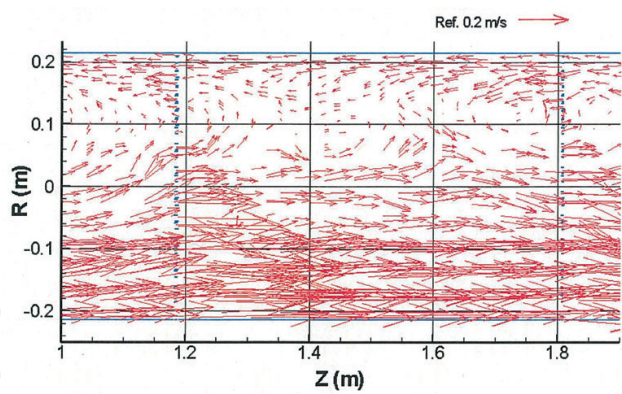**Figure 8.** Density contours at the longitudinal symmetric plane.

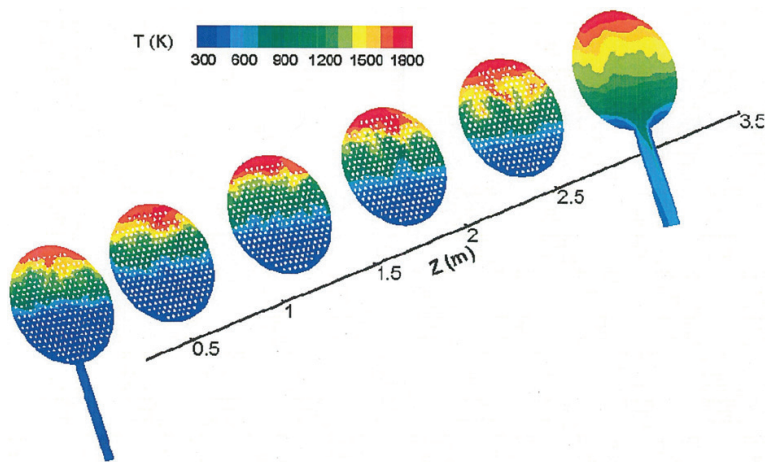**Figure 9.** Velocity vectors at part of the longitudinal symmetric plane.

Figure 10. Temperature contours at the inlet, outlet, and four middle cross sections.
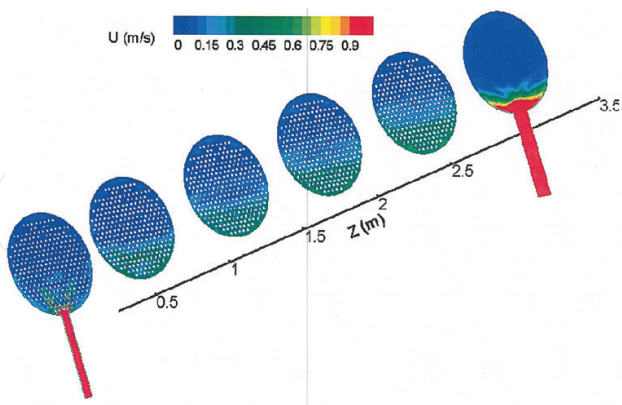

Figure 11. Velocity magnitude contours at the inlet, outlet, and four middle cross sections.

Notice that the fluid in the upper high-temperature regions is continuously heated by the heating elements that are more or less uniformly distributed over the vessel cross sections. The only way, for the fluid in these swirling regions to release some of the heat, is through diffusion (molecular and week turbulent), which is significantly less effective than convection.
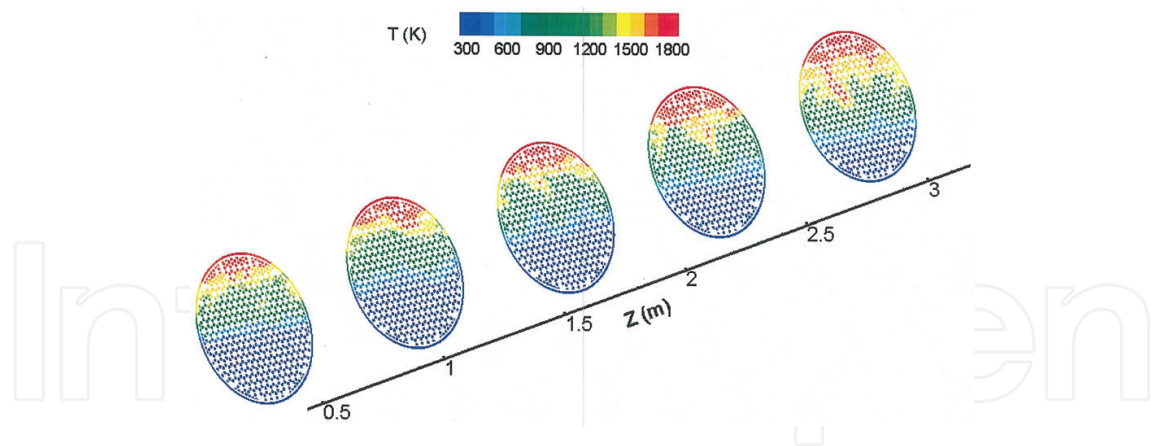
Figure 12. Temperature contours at the five keeper cross sections.
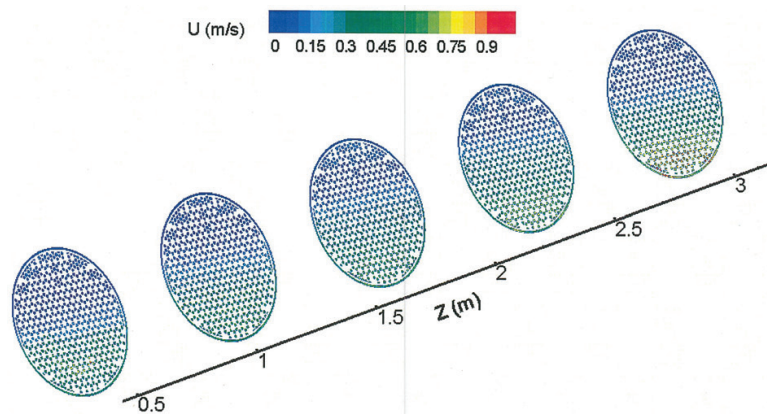

Figure 13. Velocity magnitude contours at the five keeper cross sections.
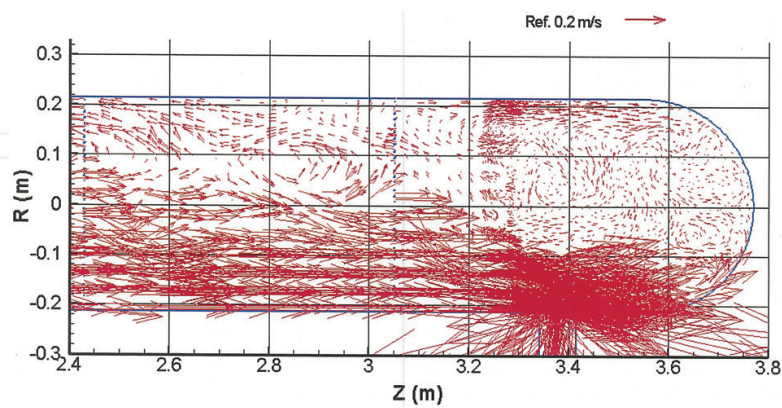

Figure 14. Velocity vectors at the downstream part of the longitudinal symmetric plane.

When the flow reaches quasi-steady, the gas temperature can be as high as ~1700 K (**Figure 4**). This is why although the mean methane temperature at the exchanger exit is increased by only ~200 K, the temperature at the top wall of the vessel can reach ~1700 K.

The above results and discussion suggest that to avoid the competition between the forced and natural convections in a perpendicular manner, the heat exchanger assembly should be mounted vertically, and to avoid fluid trapping, the flow exit pipe should be located on top of the vessel. With these arrangements, it is expected that the gravity effect or natural convection effect would be more or less uniform at each horizontal cross section, and no local high-temperature region would occur inside the heat exchanger.
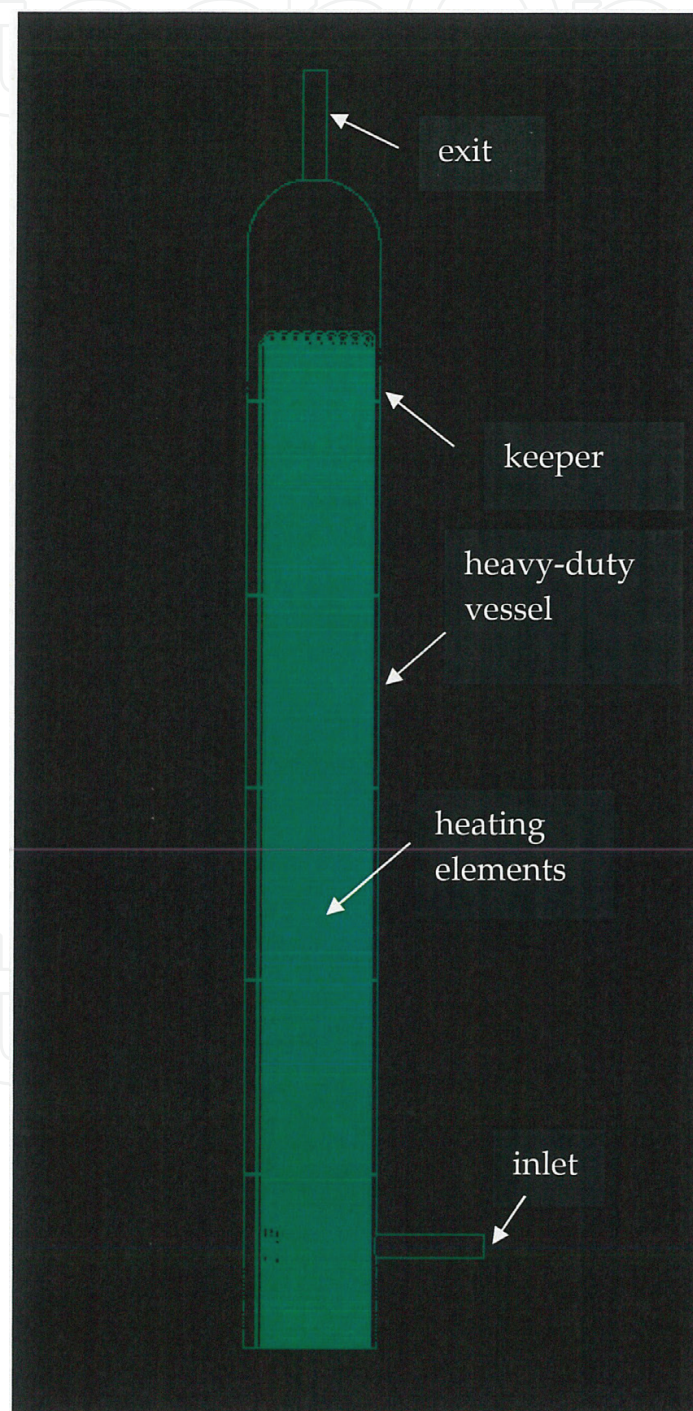

Figure 15. Modified heat exchanger configuration.

3.2. Results of the modified natural gas heat exchanger

The modified heat exchanger configuration is shown in **Figure 15**, where the whole assembly is mounted vertically and the outlet pipe is moved to the vessel top, and other parts remain the same as the original design. Similar mesh was generated for the new design, and the boundary conditions and numerical methods were unchanged.

The temperature contours along the longitudinal symmetric plane are shown in **Figure 16**. The flow temperature gradually increases from 295 K at the inlet to 495 K at the exit with an increase of 200 K. The maximum temperature is 564 K at the top surfaces of the heating elements
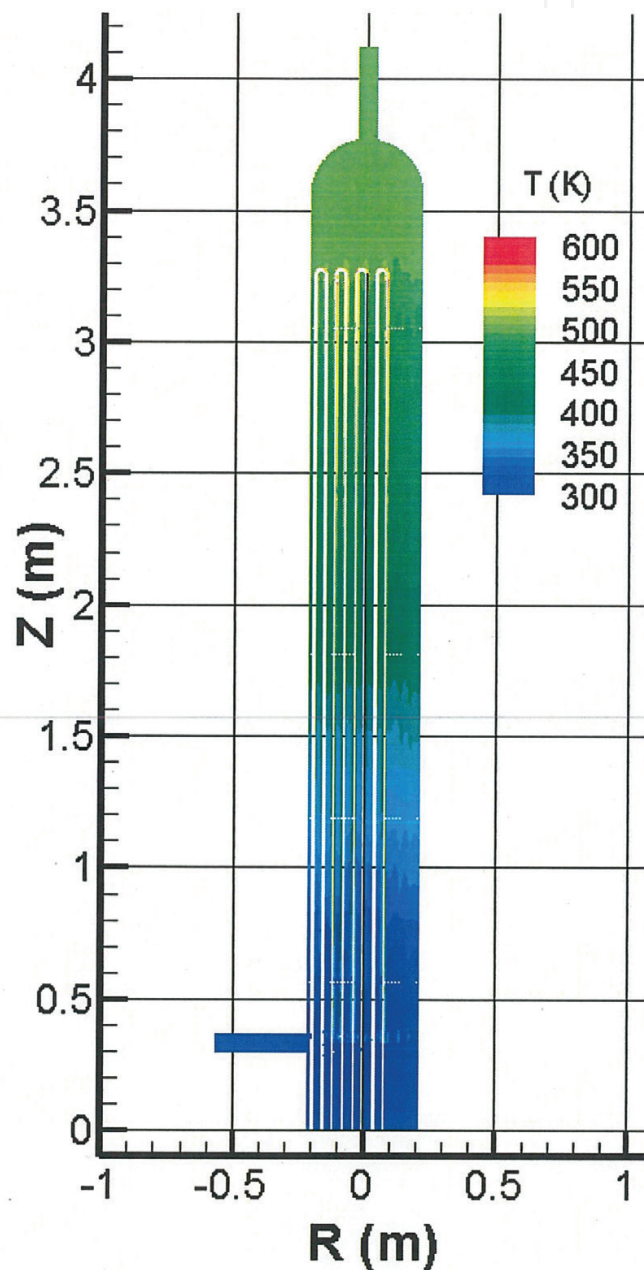

Figure 16. Temperature contours at the longitudinal symmetric plane.

(also see **Figure 21** later), and the temperature difference between the element walls and sur-rounding fluid is the driving force for heat transfer from the heat elements to the fluid. The temperature profiles at the right- and left-side walls are displayed in **Figure 17**. The wall temperature gradually increases along the vertical direction from 295 K to 495 K, and the maximum wall temperature is equal to the exit gas temperature.

Similar to the original design, the velocity magnitude shown in **Figure 18** is low inside the vessel, and its averaged value is 0.18 m/s with a maximum of 5.3 m/s at the center of the exit. The absolute pressure distribution inside the vessel also varies a little around 3.04×10^6 Pa,
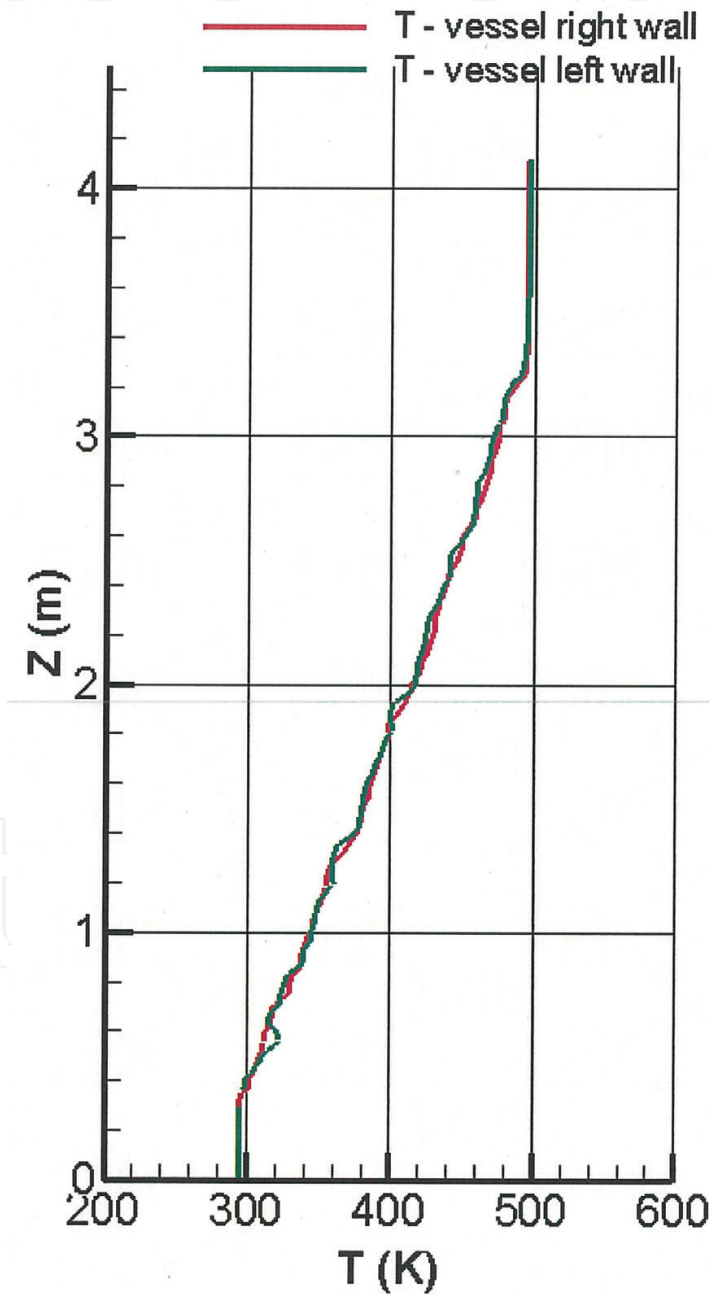

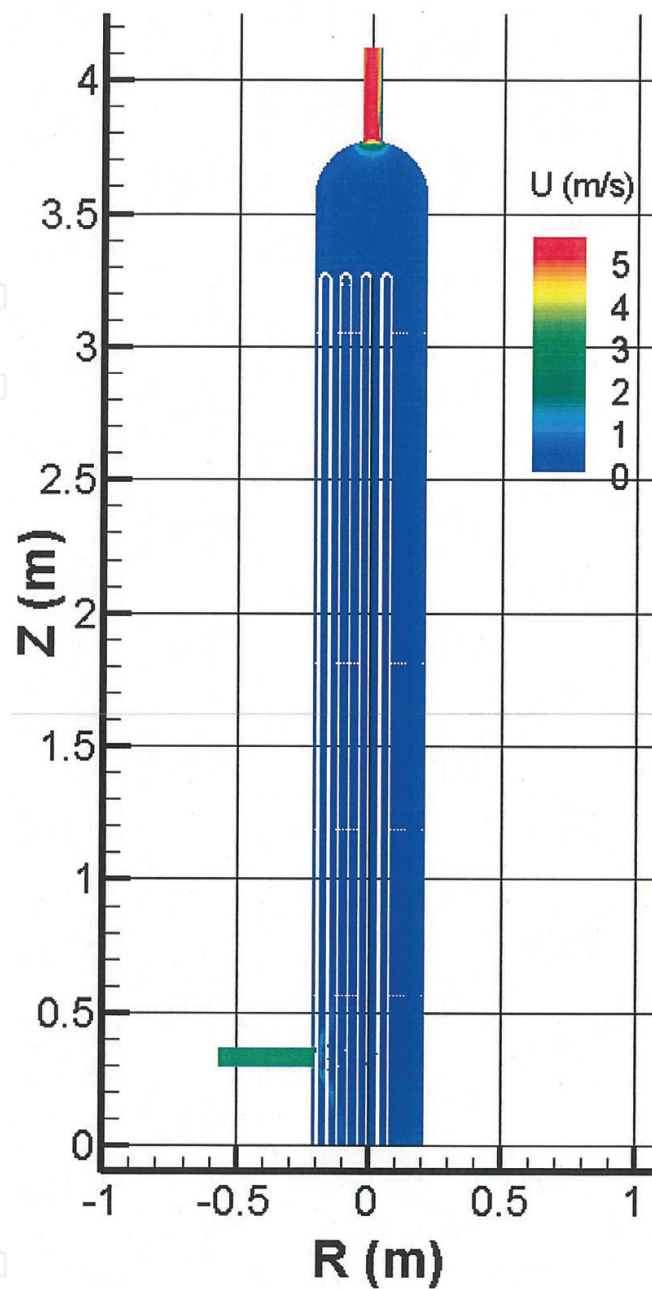**Figure 17.** Temperature profiles along the vessel right and left walls.

Figure 18. Velocity magnitude contours at the longitudinal symmetric plane.

as indicated in **Figure 19**. **Figure 20** presents the density contours at the symmetric plane. It gradually decreases from 20 kg/m^3 at the inlet to 11.8 kg/m^3 at the exit and is more or less uniform at vertical cross sections.

Detailed distributions of temperature and velocity magnitude at the inlet, five middle and exit cross sections are provided in **Figures 21** and **22**. The same parameter plots across the five keepers are given in **Figures 23** and **24**. These figures clearly indicate that the flow parameters are rather uniform at each cross section, particularly at the five keeper cross sections. The temperature gradually increases from the upstream to downstream sections, as illustrated in
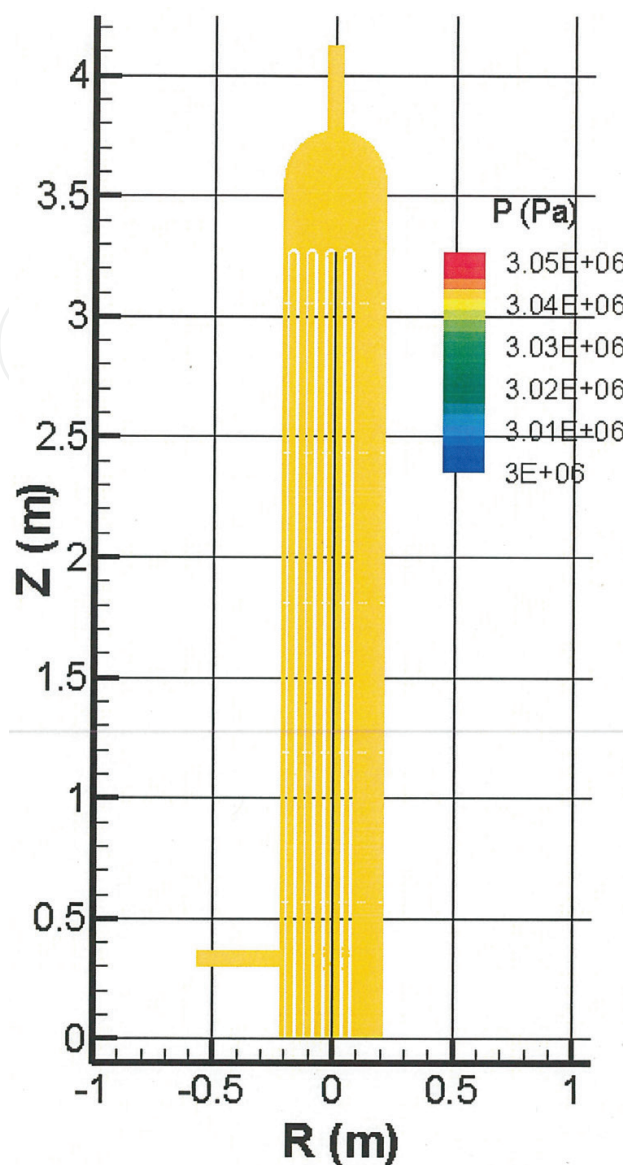
Figure 19. Absolute pressure contours at the longitudinal symmetric plane.

Figures 21 and **23**, and the maximum temperature is about 560 K. As shown in **Figure 22**, the flow velocity gradually increases from the inlet to the exit, except for small local regions at the inlet and first middle sections.

In summary, the flow features of the modified design are remarkably different from those for the original design, except that the velocity magnitude is low and the absolute pressure is about 3.4×10^6 Pa for both cases. For the modified design, both the natural and forced convections are aligned in the vertical direction; therefore, the flow parameters are more or less uniform at each vertical cross section and the flow field is stable without randomly located large recirculation regions. Moreover, the gas flows out of the exit at the required temperature and the vessel wall temperature remains the same as the surrounding gas. This proposed design has been successfully used to date.
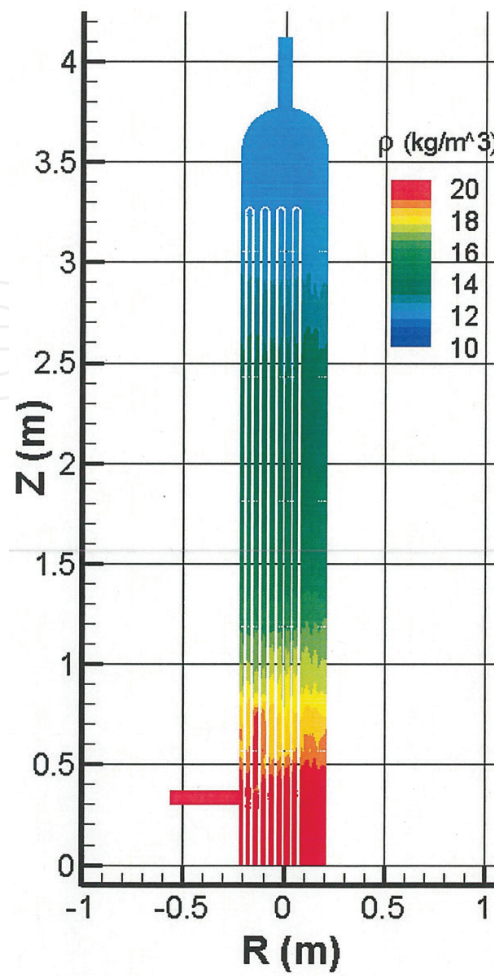
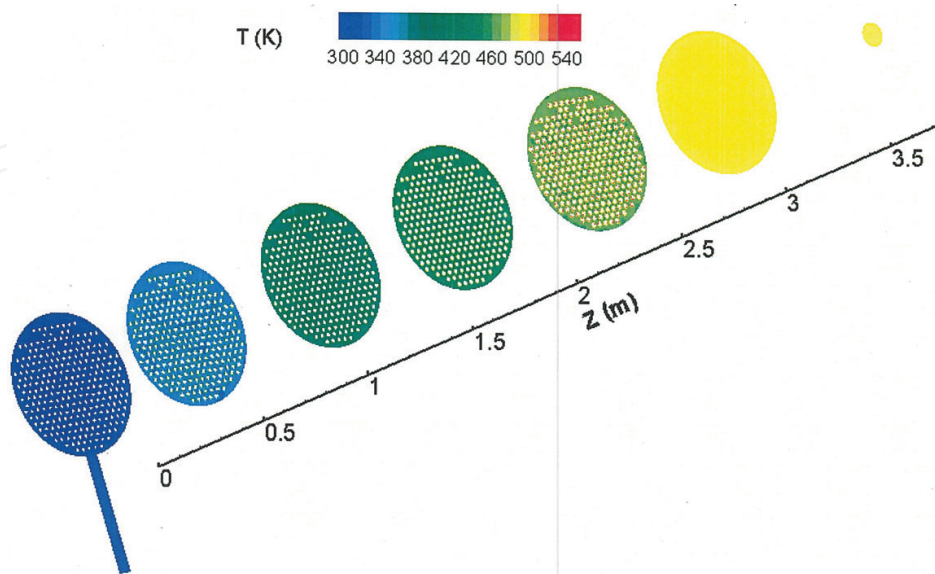**Figure 20.** Density contours at the longitudinal symmetric plane.

Figure 21. Temperature contours at the inlet, outlet, and five middle cross sections.
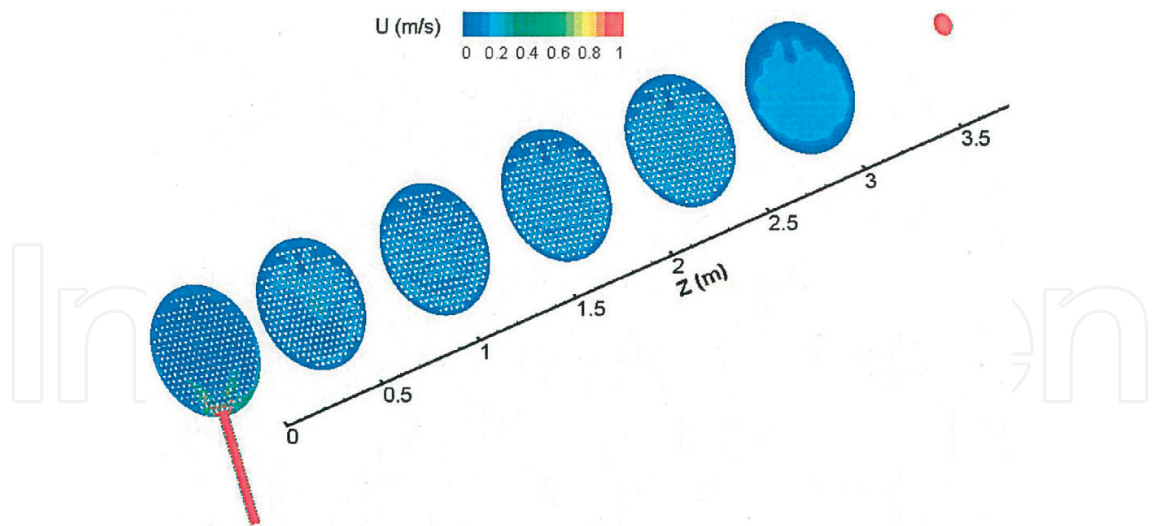
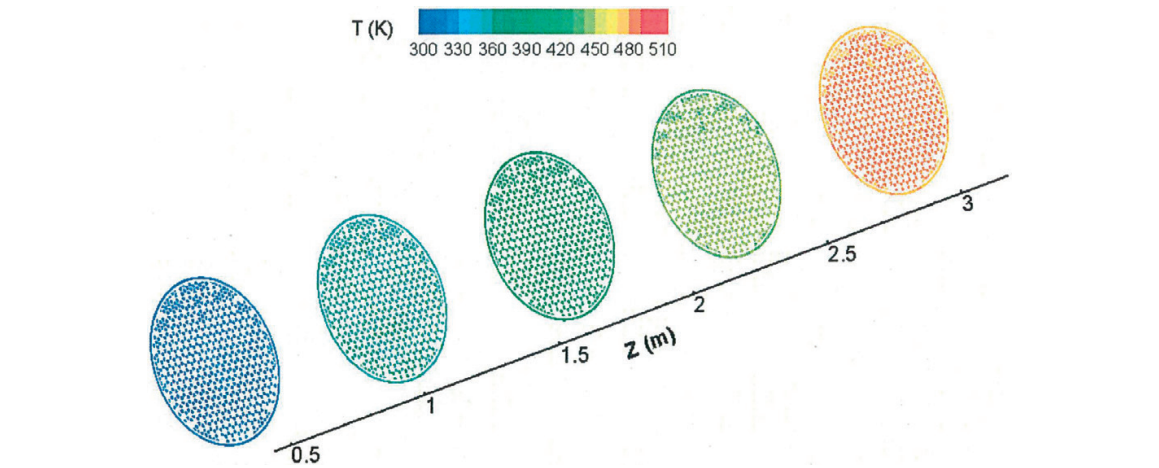**Figure 22.** Velocity magnitude contours at the inlet, outlet, and five middle cross sections.

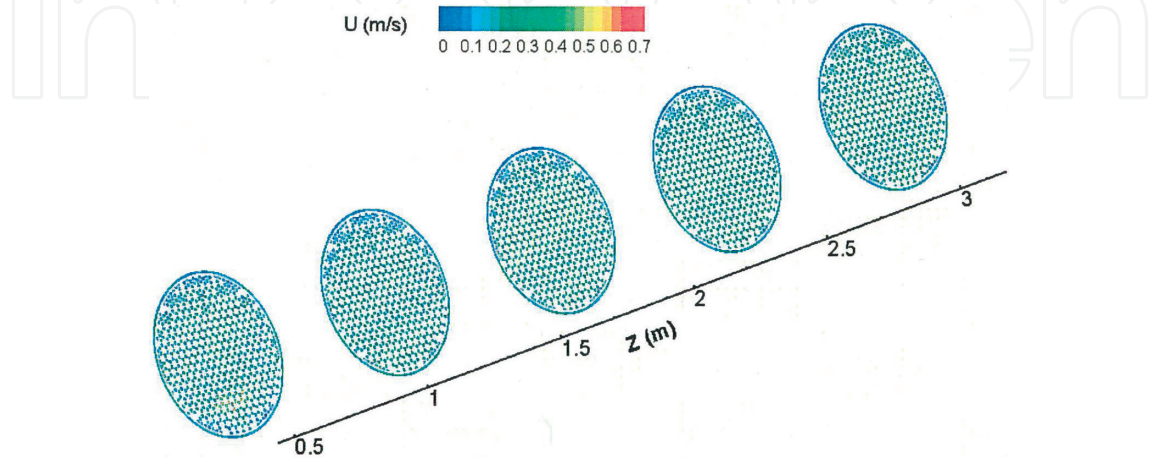**Figure 23.** Temperature contours at the five keeper cross sections.

Figure 24. Velocity magnitude contours at the five keeper cross sections.

4. Conclusions

To investigate the damage of a natural gas heat exchanger, the numerical simulations of the flow fields of the original and modified designs are performed. It is found that there are two reasons for the damage. First, at the required operating conditions, the forced convection is weak, and the natural convection is strong and comparable with the forced convection. These two actions are perpendicular and compete to each other. As a result, strong unsteadiness in the flow field is induced. Second, the whole assembly is mounted horizontally and the flow exit pipe is located at the lowest position. Consequently, the high-temperature or low-density fluid is trapped in the upper portion of the vessel. The trapped fluid is continuously heated by the heating elements located in the upper region of the vessel and eventually exceeds the allowed service temperature of the steel pipe.

The numerical results and analysis suggest that the heat exchanger assembly should be mounted vertically and the exhaust pipe should be located at the top of the exchanger. With these modifications, the flow parameters become more or less uniform at each vertical cross section, the flow field becomes stable, the methane temperature at the exit reaches the designed value, and the vessel wall temperature remains the same as the surrounding gas. This new design has been trouble-free used up to now.

Author details

Lei-Yong Jiang*, Yinghua Han, Michele Capurro and Mike Benner

*Address all correspondence to: lei-yong.jiang@nrc-cnrc.gc.ca

Aerospace, National Research Council of Canada, Ottawa, Ontario, Canada

References

[1] Poinsot T, Veynante D. Theoretical and Numerical Combustion. Philadelphia, PA: R. T. Edwards Inc.; 2005

[2] ANSYS Inc., Fluent 18.0 Documentation. Lebanon, NH, USA; 2016

[3] Jiang LY. A critical evaluation of turbulence modelling in a model combustor. ASME Journal of Thermal Science and Engineering Applications. 2013;**5**(3):031002

[4] Jiang LY, Campbell I. Reynolds analogy in combustor Modelling. International Journal of Heat and Mass Transfer. 2008;**51**(5-6):1251-1263

[5] Hinze JO. Turbulence. New York: The McGraw-Hill Book Company Inc.; 1987. p. 372-753

[6] White FM. Heat and Mass Transfer. New York: Addison-Wesley Publishing Company; 1988. p. 320-641

[7] Chase MW. National Institute of Standards and Technology (U.S.), NIST-JANAF Thermochemical Tables, 4th edition, Washington, DC, 1998

[8] Lemmon EW, McLinden MO, Huber ML. REFPROP, Reference Fluid Thermodynamic and Transport Properties, NIST Standard Reference Database 23, Version 7.0, 2002

[9] OneSteel Piping Systems. 2012. Available from: http://www.onesteelbuildingservices.com/pdffiles/OneSteel_%20Pipe_Catalogue_web.pdf

[10] Incropera FP, DeWitt DP. Fundamentals of Heat and Mass Transfer. USA: John Wiley & Sons Inc.; 2002